http://dx.doi.org/10.5935/0103-5053.20140197

J. Braz. Chem. Soc., Vol. 25, No. 11, 2080-2087, 2014.
Printed in Brazil - ©2014 Sociedade Brasileira de Química
0103 - 5053 $6.00+0.00

Article

Novel Luminescent Eu^{3+}-Indandionate Complexes Containing Heterobiaryl Ligands

João B. M. Resende Filho,[a] Jannine C. Silva,[a] Juliana A. Vale,[a] Hermi F. Brito,[b] Wagner M. Faustino,[a] José G. P. Espínola,[a] Maria C. F. C. Felinto[c] and Ercules E. S. Teotonio[,a]*

[a]*Departamento de Química, Universidade Federal da Paraíba, 58051-970 João Pessoa-PB, Brazil*

[b]*Departamento de Química Fundamental, Instituto de Química da Universidade de São Paulo, 05508-900 São Paulo-SP, Brazil*

[c]*Instituto de Pesquisas Energéticas e Nucleares, Av. Prof. Lineu Prestes, 2242, Cidade Universitária, 05508-000 São Paulo-SP, Brazil*

Novos complexos indandionatos de fórmulas $[Ln(aind)_3L(H_2O)]$ e $[Ln(bind)_3L]\cdot H_2O$, (L: 1,10-fenantrolina (phen) ou 4,7-dimetil-1,10-fenantrolina (dmphen), Ln^{3+}: Eu^{3+} ou Gd^{3+}, aind: 2-acetil-1,3-indandionato e bind: 2-benzoil-1,3-indandionato) foram sintetizados e caracterizados por análise elementar, espectroscopia de absorção na região do infravermelho e análise termogravimétrica. Os dados de caracterização são consistentes com a presença de uma molécula de água de cristalização nas estruturas dos compostos $[Ln(bind)_3L]\cdot H_2O$, enquanto que nos complexos $[Ln(aind)_3L(H_2O)]$ a molécula de água atua como ligante. As geometrias dos complexos do íon Eu^{3+}, otimizadas pelo modelo SPARKLE/AM1, foram consistentes com os resultados experimentais de luminescência. As propriedades luminescentes dos compostos de Eu^{3+} são discutidas em termos de parâmetros de intensidade experimentais (Ω_2 e Ω_4), taxas radiativas (A_{rad}) e não-radiativas (A_{nrad}) e eficiência quântica de emissão (η). Os maiores valores de η foram obtidos para os compostos $[Eu(bind)_3L]\cdot H_2O$, refletindo a ausência de moléculas de água na primeira esfera de coordenação do íon Eu^{3+}.

Novel Ln^{3+}-indandionate complexes of formulas $[Ln(aind)_3L(H_2O)]$ and $[Ln(bind)_3L]\cdot H_2O$ (L: 1,10-phenanthroline (phen) or 4,7-dimethyl-1,10-phenanthroline (dmphen), Ln^{3+}: Eu^{3+} or Gd^{3+}, aind: 2-acetyl-1,3-indandionate and bind: 2-benzoyl-1,3-indandionate) were synthesized and characterized by elemental analysis, infrared spectroscopy, and thermogravimetric analyses. The characterization data are consistent with the presence of a water lattice molecule in the $[Ln(bind)_3L]\cdot H_2O$ compounds. However, the data also suggest that the water acts as a coordinated molecule in the $[Ln(aind)_3L(H_2O)]$ ones. Theoretical geometries of the Eu^{3+}-complexes have been optimized via the SPARKLE/AM1 Model for lanthanide complexes that are consistent with their luminescence experimental data. The photoluminescence properties of the Eu^{3+}-compounds have been discussed in terms of experimental intensity parameters (Ω_2 and Ω_4), radiative (A_{rad}), and non-radiative (A_{nrad}) spontaneous emission coefficients. The higher values of emission quantum efficiency (η) of the $[Eu(bind)_3L]\cdot H_2O$ compounds reflect the absence of luminescence-quenching water molecule in their first coordination spheres.

Keywords: lanthanides, 2-acyl-1,3-indandionates, 4,7-dimethyl-1,10-phenanthroline

Introduction

2-acyl-1,3-indandiones (acind) compounds have been frequently used as precursor's molecules for the synthesis of novel compounds exhibiting biological activities and spectroscopic properties.[1-3] They are well known for their microbial, anti-tumor, anti-inflammatory, anticoagulants, herbicides, and insecticide activities.[4,5] Therefore, 2-acyl-1,3-indandiones have been inspired intensive theoretical and experimental investigations.[6-11]

The significant interest in the investigation of the indandionate complexes has been increased in the last decade.[6-12] This kind of cyclic ligands presents a good chelating ability owing to the existence of three carbonyl

*e-mail: teotonioees@quimica.ufpb.br

groups, which has contributed to obtain different d-metal complexes with high thermodynamic and photophysical stabilities. Most of the studies on d-metal complexes with the acind ligand have been concerned with structural and magnetic properties.[6-10] However, there are only a few works reporting on Ln^{3+}-complexes with these ligands, for example, the first structural characterization and photoluminescent as well as electroluminescent properties of the Ln^{3+}-complexes containing 2-acyl-1,3-indandionates ligands have been reported by our group.[11,12] Moreover, Li *et al.*[13] have reported similar study on the Eu^{3+}-complexes containing the 2-(2,2,2-trifluoroacethyl)-1-indone (TFI) ligand, which presents correlated structure with the 2-acyl-1,3-indandionate ligands.

Lanthanide diketonate complexes containing heterobiaryl ligands have been the subject of extensive studies in the literature ranging from synthesis, characterization, and their photoluminescent properties to sensor applications.[14-17] Although the great coordinating ability of bidentate 1,10-phenanthroline and 4,7-dimethyl-1,10-phenanthroline ligands through the two nitrogen atoms to the Ln^{3+} ions, up to now, to our knowledge, no work has been reported on luminescent properties of complexes containing indandionate and heterobiaryl as ancillary ligands. Furthermore, the relatively rigid structure of the heteroaryl ancillary ligands may contribute to minimize the luminescence quenching of the europium ion via thermal vibrations.

Based on the above considerations, in this work, we have reported the synthesis and spectroscopic studies of the novel $[Ln(aind)_3(L)(H_2O)]$ and $[Ln(bind)_3(L)]\cdot H_2O$ complexes, where aind = 2-acetyl-1,3-indandione, bind = 2-benzoyl-1,3-indandione, Ln = Eu^{3+} or Gd^{3+}, and L = 1,10-phenanthroline or 4,7-dimethyl-1,10-phenanthroline (Figure 1). In addition, theoretical structures of the Eu^{3+} complexes were optimized by semi-empirical quantum-mechanical calculations and their optical properties have been investigated on the basis of experimental intensity parameters.

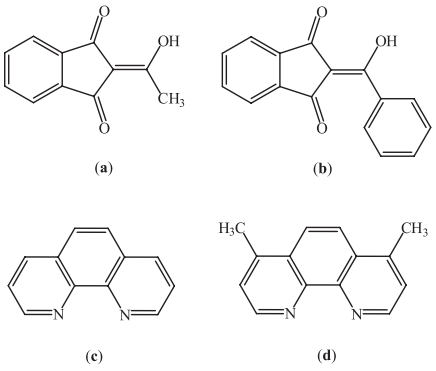

Figure 1. Structural formulas of the ligands: (a) 2-acetyl-1,3-indandione (aind), (b) 2-benzoyl-1,3-indandione (bind), (c) 1,10-phenanthroline (phen), and (d) 4,7-dimethyl-1,10-phenanthroline (dmphen).

Experimental

Materials and methods

The solvents (acetone and ethanol), 1,10-phenanthroline, 4,7-dimethyl-1,10-phenanthroline and lanthanide oxides (Ln_2O_3) were purchased from Aldrich Co. and used without previous treatment. Hexahydrated lanthanide chlorides, $LnCl_3\cdot 6H_2O$, were prepared by reaction between Ln_2O_3 and hydrochloric acid purchased from Aldrich Co.[18] 2-acetyl-1,3-indandione (aind), 2-benzoyl-1,3-indandione (bind) ligands, and $[Ln(aind)_3(H_2O)_2]$, $[Ln(bind)_3(H_2O)_2]$ precursor complexes were synthesized according to the procedures as reported in the literature.[4,11]

Elemental analyses (C, H, and N) were carried out using a Perkin Elmer 2400 elemental microanalyzer. Infrared (IR) spectra were recorded from 400 to 4000 cm^{-1} on a Shimadzu FT-IR spectrophotometer model IRPRESTIGE-21 using KBr pellets. Excitation and emission spectra of the Ln^{3+}-complexes in solid state were recorded at liquid nitrogen temperature on a Fluorolog-3 spectrofluorometer (Horiba) with excitation and emission double grating 0.22 m monochromators, and a 450 W Xenon lamp as excitation source and R928P PMT as detector. All spectra were recorded using a detector mode correction. The second-order diffraction of the source radiation was eliminated using a cut-off filter. Luminescence decay curves of the Eu^{3+}-complexes in the solid state were recorded at low temperature (77 K) using the same equipment but operating on the phosphorescence mode with pulsed Xenon lamp as excitation source. The luminescence instruments were fully controlled by the FluorEssence program. All the luminescence data of the samples were measured in quartz tube of 2 mm in diameter. TG curves were recorded from 30 to 900 °C using a Shimadzu DTG-60H thermobalance with a heating rate 10 °C min^{-1} under a nitrogen atmosphere.

Synthesis of the Ln^{3+}-complexes with heteroaromatic ligands

Lanthanide indandionate complexes containing ancillary ligands were synthesized by mixing acetonic solutions of the corresponding hydrated complexes, $[Ln(aind)_3(H_2O)_2]$ or $[Ln(bind)_3(H_2O)_2]$, with phen or dmphen ligands in the molar ratio of complex:ligand (1:1.3). The resulting solutions were stirred for 1 h at room temperature (ca. 27 °C). Later on, these solutions were stand up until the total evaporation of solvent. The prepared

yellow solids were washed thoroughly with cold ethanol and dried under reduced pressure.

[Eu(aind)$_3$(phen)(H$_2$O)] (**1**): 0.2482 g, yield 68%; FT-IR (KBr, cm^{-1}): 3485(w), 3443(w), 3057(w), 2951(w), 2920(w), 2856(w), 1681(m), 1643(m), 1622(s), 1585(s), 1467(s), 1363(m), 1340(m), and 732(s). Anal. Calc. for $C_{45}H_{31}EuN_2O_{10}$: C, 59.28, H, 3.43, and N, 3.07. Found: C, 59.71; H, 3.35, and N, 2.74.

[Eu(bind)$_3$(phen)]·H$_2$O (**2**): 0.4230 g, yield 72%; FT-IR (KBr, cm^{-1}): 3429(w), 3055(w), 2952(w), 2920(w), 1694(m), 1618(s), 1587(s), 1568(s), 1564(s), 1448(s), 1420(s), 1340(m), and 741(m). Anal. Calc. for $C_{60}H_{37}EuN_2O_{10}$: C, 65.64; H, 3.40, and N, 2.55. Found: C, 65.35, H, 3.44, and N, 2.84.

[Gd(aind)$_3$(phen)(H$_2$O)] (**3**): 0.2088 g, yield 56%; FT-IR (KBr, cm^{-1}): 3524(w), 3433(w), 3057(w), 2951(w), 2922(w), 2866(w), 2856(w), 1682(m), 1643(m), 1622(s), 1587(s), 1467(s), 1364(m), 1340(m), and 735(s). Anal. Calc. for $C_{45}H_{31}GdN_2O_{10}$: C, 58.94, H, 3.41, and N, 3.05. Found: C, 59.63, H, 4.15, and N, 2.66.

[Gd(bind)$_3$(phen)]·H$_2$O (**4**): 0.2042 g, yield 58%; FT-IR (KBr, cm^{-1}): 3445(w), 3053(w), 3032(w), 2926(w), 1694(m), 1636(m), 1616(s), 1587(s), 1568(s), 1564(s), 1448(s), 1423(s), 1340(m), and 741(m). Anal. Calc. for $C_{60}H_{37}GdN_2O_{10}$: C, 65.32, H, 3.38, and N, 2.54. Found: C, 65.55, H, 3.34, and N, 3.24.

[Eu(aind)$_3$(dmphen)(H$_2$O)] (**5**): 0.1050 g, yield 57%; FT-IR (KBr, cm^{-1}): 3564(w), 3502(w), 3068(w), 1691(m), (s), 1643(s), 1620 (s), 1583(s), 1467(s), 1359(m), 1340(m), and 725(s). Anal. Calc. for $C_{47}H_{35}EuN_2O_{10}$: C, 60.06, H, 3.73, and N, 2.98. Found: C, 60.26, H, 3.71, and N, 3.01.

[Eu(bind)$_3$(dmphen)]·H$_2$O (**6**): 0.1030 g, yield 58%; FT-IR (KBr, cm^{-1}): 3435(w), 3055(w), 1693(m), 1629(m), 1612(m), 1585(s), 1564(s), 1448(s), 1421(s), 1361(m), and 736(m). Anal. Calc. for $C_{62}H_{41}EuN_2O_{10}$: C, 66.13, H, 3.64, and N, 2.49. Found: C, 66.28, H, 3.48, and N, 2.52.

[Gd(aind)$_3$(dmphen)(H$_2$O)] (**7**): 0.1630 g, yield 60%; FT-IR (KBr, cm^{-1}): 3442(w), 3068(w), 1685(m), 1645(m), 1620(s), 1585(s), 1467(m), 1357(m), 1340(m), and 729(m). Anal. Calc. for $C_{47}H_{35}GdN_2O_{10}$: C, 59.74, H, 3.71, and N, 2.97. Found: C, 60.32, H, 3.61, and N, 3.12.

[Gd(bind)$_3$(dmphen)]·H$_2$O (**8**): 0.0980 g, yield 55%; FT-IR (KBr, cm^{-1}): 3441(w), 3053(w), 1691(m), 1629(s), 1612(s), 1585(s), 1564(s), 1450(s), 1421(s), 1342(m), and 736(m). Anal. Calc. for $C_{62}H_{41}GdN_2O_{10}$: C, 65.84, H, 3.63, and N, 2.47. Found: C, 65.92, H, 3.57, and N, 2.67.

Results and Discussion

Characterization

The results of the elemental analysis (C, H, and N) are consistent with the monohydrated formulas of Ln(aind)$_3$L·H$_2$O and Ln(bind)$_3$L·H$_2$O complexes, where Ln = Eu^{3+} or Gd^{3+}.

The infrared spectra of the Ln^{3+}-complexes (Figure 2) exhibit two bands at around 1560 and 1690 cm^{-1} assigned to the ν(C=O) stretching modes, due to the coordinated and non-coordinated carbonyl groups, respectively. These data are in agreement with the FT-IR spectral data of precursor-hydrated complexes,[11] suggesting that the 2-acyl-1,3-indandione ligands are coordinated to Ln^{3+} ions through oxygen atoms of the carbonyl groups in bidentate mode. Moreover, the absorption bands at around 1468 and 1423 cm^{-1} indicate that the phen and dmphen ligands act as chelating agents, coordinating to the Ln^{3+} ion through the nitrogen atoms.[19,20] The complexes also exhibit absorption bands in the spectral range 4000-3200 cm^{-1} assigned to ν(O–H) stretching of the water molecule (Figure 2). Interestingly, FT-IR spectra of the [Ln(aind)$_3$L·H$_2$O] compounds exhibit narrow peaks at around 3560 cm^{-1}, while the [Ln(bind)$_3$L]·H$_2$O compounds show only one broad absorption band. These data give

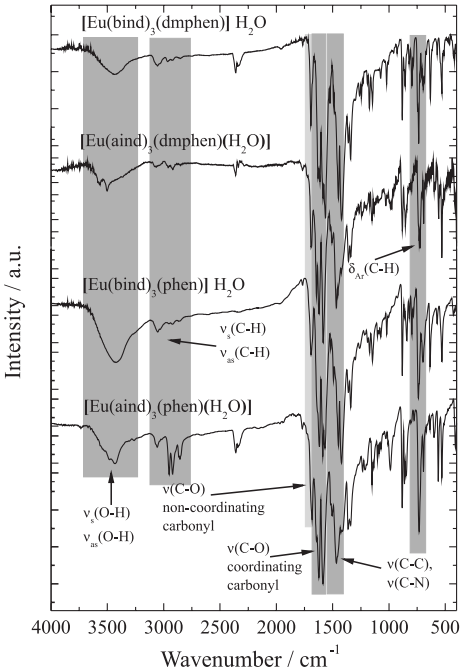

Figure 2. FT-IR absorption spectra of the Eu^{3+}-complexes recorded in the range of 4000-400 cm^{-1} in KBr pellets.

evidences that the water molecule is coordinated to the Ln^{3+} ion only in the $[Ln(aind)_3L{\cdot}H_2O]$ complexes. Similar spectral profiles have also been observed for La^{3+} and Tb^{3+} complexes using EDTA as ligand that present coordinated and non-coordinated water molecules, respectively.[21,22]

Thermogravimetric curves of the $[Eu(aind)_3(dmphen)(H_2O)]$ and $[Eu(bind)_3(dmphen)]{\cdot}H_2O$ compounds (Figure 3) show that these systems undergo thermal decomposition in consecutive steps. The curves show the first weight loss in the temperature range from 60 to 110 °C that correspond to 1.6% for $[Eu(bind)_3(dmphen)]{\cdot}H_2O$ and 2.1% for $[Eu(aind)_3(dmphen)(H_2O)]$, which are in agreement with the release of water molecules. However, it can be observed in Figure 3 that the $[Eu(aind)_3(dmphen)(H_2O)]$ complex exhibits a shorter dehydration interval (60-130 °C) than the $[Eu(bind)_3(dmphen)](H_2O)$ complex, in which the dehydration process occurs from 40 to 150 °C (see insert Figure 3). These data corroborate with the FT-IR results, indicating that the water molecules are acting as ligand in the former complex. Similar behavior has been observed in the thermal and FT-IR studies of the Ln^{3+}-EDTA complexes, as reported by Gigante *et al.*.[22]

Figure 3 also shows that the anhydrous compounds undergo consecutive weight loss starting from 250 °C, yielding the lanthanide oxides, for example, Eu_2O_3, that is in agreement with theoretical values: 15.3% (calc. 18.7%) and 16.4% (calc. 15.6%) for $[Eu(aind)_3(dmphen)(H_2O)]$ and $[Eu(bind)_3(dmphen)]{\cdot}H_2O$ compounds, respectively.

Theoretical structural studies

Theoretical molecular structures of the $[Eu(aind)_3L(H_2O)]$ and $[Eu(bind)_3L]{\cdot}H_2O$ complexes, where L = phen or dmphen, were optimized using the reparameterized latest version of the SPARKLE/AM1 model for Eu(III) and other lanthanide ions implemented in the software package MOPAC2012.[23,24]

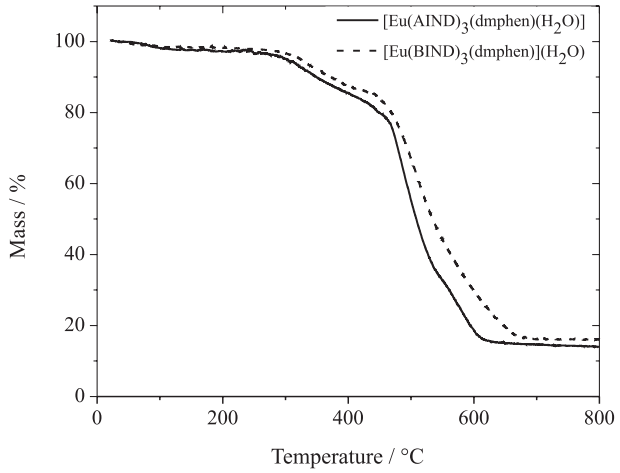

Figure 3. Thermogravimetric curves of the $[Eu(aind)_3(dmphen)(H_2O)]$ (solid line) and $[Eu(bind)_3(dmphen)]{\cdot}H_2O$ (dashed line) complexes.

Water molecule was not considered in the last complexes, since the FT-IR and thermogravimetric data indicate that the water molecule is out of the first coordination sphere. The calculated structures of the $[Eu(aind)_3(dmphen)(H_2O)]$ and $[Eu(bind)_3(dmphen)]{\cdot}H_2O$ complexes are shown in Figure 4, while those ones for the similar complexes with phen ligand are presented in Supporting Information (Figure S1).

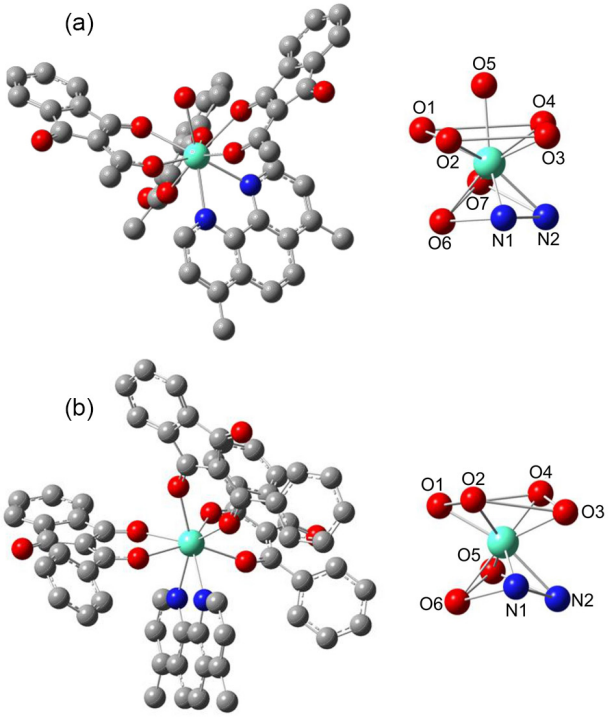

Figure 4. Theoretical geometries of the Eu^{3+}-complexes optimized by the SPARKLE/AM1 model: (a) $[Eu(aind)_3(dmphen)(H_2O)]$ and (b) $[Eu(bind)_3(dmphen)]{\cdot}H_2O$.

The optimized structures reveal that the indandionate ligands are characterized by the planarity of 1,3-indandione moieties. In addition, the substituent phenyl groups in the bind ligands are twisted from the 1,3-indandione moieties at around angles of 29 and 40°. The less pronounced twist is observed in the phenyl group that belongs to the bonded molecule more distant from heteroaromatic ligand. This behavior reflects the steric hindrance on the ligands due to the heteroaromatic one in the first coordination sphere. Thus, the phenyl groups are orientated to minimize steric repulsion among ligands. Therefore, the steric hindrance due to the substituent phenyl groups of the ligand is enough to avoid water coordination to the lanthanide ion compared to the $[Eu(aind)_3L(H_2O)]$ complexes.

The coordination polyhedron, EuN_2O_6, for the $[Eu(bind)_3L]{\cdot}H_2O$ complexes can be described as distorted

square antiprismatic geometries (Figure 4b, Figure S1). A square face contains four oxygen atoms from indandionate ligands, another one presenting two oxygen atoms from indandionate and two nitrogen atoms belong to phen or dmphen ligand.

The coordination polyhedron of the $[Eu(aind)_3L(H_2O)]$ complex, EuN_2O_7, is better described as a distorted monocapped square antiprismatic geometry, with oxygen atom from water molecule occupying the capping position (Figure 4a, Figure S1). The bond lengths of Eu^{3+}-O(indandionate), and Eu^{3+}-N(heteroaromatic) in the complexes are around 2.38 and 2.51 Å, respectively. These structural data are close to those obtained for $[Eu(isovind)_3(EtOH)(H_2O)]$,[11] as well as other Eu^{3+}-compounds with bipy and phen ligands.[25-28]

Photoluminescent properties of the Gd^{3+}-compounds

The phosphorescence spectra of the analogous $[Gd(aind)_3L(H_2O)]$ and $[Gd(bind)_3L]\cdot H_2O$ compounds were recorded at 77 K with excitation monitored at 370 nm for $S_0 \rightarrow S_1$ transition, in order to estimate the triplet state energies (T_1) of the indandionate ligands. The Gd^{3+}-compounds were used for this propose because the lowest excited energy level of Gd^{3+} ion ($^6P_{7/2}$) is too high to receive energy from the ligands. In addition, the Gd^{3+} radius is similar to the Eu^{3+} ion, therefore, Gd^{3+}-complexes mimetize both geometry and intraligand energy level structures of Eu^{3+}-complexes. Figure S2 shows the phosphorescence spectra of the Gd^{3+}-compounds, which exhibit broad emission bands in the spectral range from 440 to 650 nm assigned to the $T \rightarrow S_0$ transition centered on the indandionate ligands.

The first T_1 excited state energies of the ligands were estimated as the energies correspond to the 0-0 phonon transitions from the phosphorescence spectra of the $[Gd(aind)_3L(H_2O)]$, and $[Gd(bind)_3L]\cdot H_2O$ compounds with values of 21906 cm^{-1} (456.5 nm), and 22371 cm^{-1} (447.0 nm), respectively. These results suggest that both the aind and bind ligands have appropriated T_1 state energies, which play most important role in intramolecular ligand-to-metal energy transfer process. Although, the S_1 and T_1 energy levels of the 1,10-phenanthroline ligand and its derivative are usually located at around 30000 and 22000 cm^{-1}, respectively,[29] the main role of these ligands in lanthanide diketonate complexes is only to act as ancillary ones.[30]

Photoluminescent properties of the Eu^{3+}-compounds

Figure 5 shows the excitation spectra of the $[Eu(aind)_3L(H_2O)]$ and $[Eu(bind)_3L]\cdot H_2O$ compounds recorded at 77 K in the spectral range 250-590 nm with emission monitored on the $^5D_0 \rightarrow {}^7F_2$ hypersensitive transition at 611 nm. These spectra are dominated by two intense broad absorption bands in the spectral range from 270-470 nm, which are assigned to the $S_0 \rightarrow S_1$ and $S_0 \rightarrow S_2$ transitions centered on the acind ligands. These bands are overlapped with the absorption bands assigned to the $S_0 \rightarrow S_1$ transition of the phen and dmphen ligands at 300 nm. The spectral profiles of the Eu^{3+}-compounds (Figure 5) indicate that the $S_0 \rightarrow S_1$ and $S_0 \rightarrow S_2$ transitions are approximately located in the 1,3-indandionate moieties. These results are in agreement with those ones observed for similar complexes, as reported in the literature.[11]

Figure 5 also presents some characteristic narrow absorption bands assigned to the $^7F_0 \rightarrow {}^{2S+1}L_J$ intraconfigurational transitions of the Eu^{3+} ion. These bands exhibit lower intensity than those ones, which correspond to the intraligand transitions, corroborating the efficient sensitization process via antenna effect.

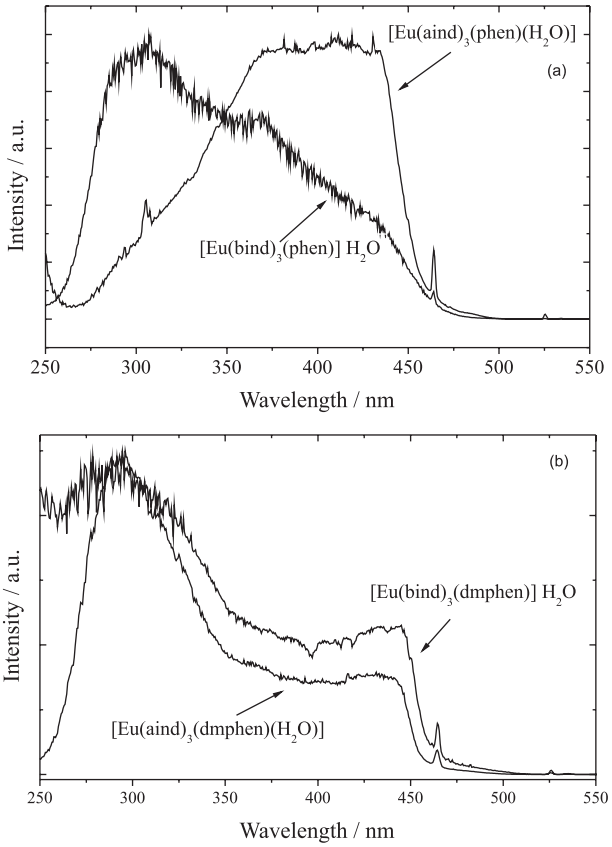

Figure 5. Excitation spectra of the Eu^{3+}-compounds recorded at 77 K in the spectral range 250-550 nm, under emission at around 612 nm. (a) $[Eu(aind)_3(phen)(H_2O)]$ and $[Eu(bind)_3(phen)]\cdot H_2O$ and (b) $[Eu(aind)_3(dmphen)(H_2O)]$ and $[Eu(bind)_3(dmphen)]\cdot H_2O$.

The emission spectra of the $[Eu(aind)_3L(H_2O)]$ and $[Eu(bind)_3L]\cdot H_2O$ compounds were recorded at 77 K in

the spectral range from 420 to 730 nm, under excitation centered on indandionate ligand, $S_0 \rightarrow S_1$ transitions (at 370 nm), as shown in Figure 6. The luminescent spectra display only the characteristic emission narrow bands that are assigned to the $^5D_0 \rightarrow {}^7F_J$ transitions of the Eu^{3+} ion, where J = 0, 1, 2, 3, and 4.[31,32]

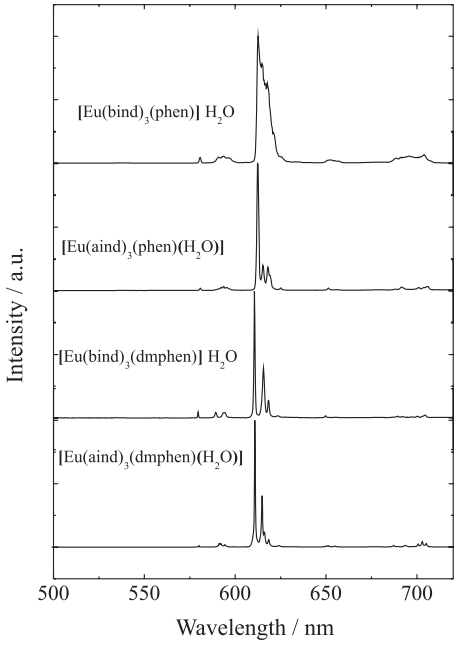

Figure 6. Emission spectra of the Eu^{3+}-complexes recorded at 77 K in the spectral range of 420-720 nm, under excitation at 370 nm.

The local ligand field effect of the Eu^{3+}-complexes has been qualitatively investigated based on the splitting and relative emission intensities of the $^5D_0 \rightarrow {}^7F_{J(0-4)}$ transitions. Table 1 presents the intraconfigurational-$4f^6$ transitions and their Stark (2J + 1)-components. The presence of the only one emission band assigned to $^5D_0 \rightarrow {}^7F_0$, as well as three stark components for $^5D_0 \rightarrow {}^7F_1$ indicate that the Eu^{3+} is located at low symmetry environment (C_n, C_{nv} or C_s).[33] These optical data corroborate with the fact that the intensity of the band assigned to $^5D_0 \rightarrow {}^7F_2$ transition is higher than that of the assigned to $^5D_0 \rightarrow {}^7F_1$ one,[27] which are in close agreement with the distorted coordination polyhedra obtained from theoretical modeling for both Eu^{3+}-complexes (Figure 4, Figure S1).

The absence of broad phosphorescence bands arising from the indandionate ligands (Figure 6) emphasizes the presence of an efficient luminescence sensitization occurring via antenna effect. The efficient intramolecular energy transfer mechanism from aind and bind ligands to the Eu^{3+} ion in the complexes is characterized by: (*i*) strong absorption of $S_0 \rightarrow S_1$ transition of the 2-acyl-1,3-indandione ligands; (*ii*) intersystem cross by the non-radiative processes $S_1 \rightarrow T$; (*iii*) energy transfer of the $T_1 \rightarrow (^5D_1, {}^5D_0)$, and (*iv*) efficient radiative process from the $^5D_0 \rightarrow {}^7F_{J(0-4)}$ transitions.[34-35]

Judd-Ofelt intensity parameters (Ω_λ = 2.4), radiative (A_{rad}), non-radiative (A_{nrad}) rates, and emission quantum efficiency (η) of the $^5D_0$ emitting level of the Eu^{3+} complexes have been quantitatively obtained from the luminescence decay curves and emission spectral data (Table 2). The luminescence decay curves (Figure S3) were recorded by monitoring the emission intensity of the hypersensitive $^5D_0 \rightarrow {}^7F_2$ transition under excitation of the $S_0 \rightarrow S_1$ transition centered on the 2-acyl-1,3-indandionate ligands at 370 nm. The curves were well-adjusted to a single exponential function, yielding the $^5D_0$ lifetimes values (τ) equal to 0.459, 0.465, 0.229, and 0.594 ms for $[Eu(aind)_3(phen)(H_2O)]$, $[Eu(bind)_3(phen)]\cdot H_2O$, $[Eu(aind)_3(dmphen)(H_2O)]$ and $[Eu(bind)_3(dmphen)]\cdot H_2O$ (Table 2), respectively. While using these data, the total decay rates were determined according to the expression: $A_{total} = 1/\tau$. The radiative rates (A_{rad}) were determined using the $^5D_0 \rightarrow {}^7F_{2,4}$ transitions (forced electric dipole) and the $^5D_0 \rightarrow {}^7F_1$ transition (magnetic-dipole) as internal reference.[36,37] The values of both radiative and noradiative rates for $[Eu(aind)_3L(H_2O)]$, and $[Eu(bind)_3L]\cdot H_2O$ complexes are presented in Table 2. When τ values of these complexes were compared with the corresponding ones of precursor hydrated complexes, it was observed a considerable decrease in both A_{rad} and A_{nrad} rates. The decrease in A_{nrad} values might be attributed to the water molecules substitution by the auxiliary phen and dmphen ligands in the first coordination sphere of the Eu^{3+} ion (Table 2), that reduce the multiphonon decays,

Table 1. Energy levels of the Eu^{3+}-complexes assigned to the transitions ($^5D_0 \rightarrow {}^7F_J$, J = 0-4) (in cm^{-1})

Transition	Eu^{3+}-complexes			
	(**1**)	(**5**)	(**2**)	(**6**)
$^5D_0 \rightarrow {}^7F_0$	17218	17253	17218	17241
$^5D_0 \rightarrow {}^7F_1$	16886; 16844; 16793	16972; 16835	16929; 16852; 16784	16915; 16886; 16722
$^5D_0 \rightarrow {}^7F_2$	16332; 16252; 16181; 16150	16377; 16244; 16175	16324; 16268; 16181; 16103	16372; 16265; 16228; 16171
$^5D_0 \rightarrow {}^7F_3$	15354; 15249; 15221	15394; 15272; 15239	15333; 15284; 15221	15380; 15356; 15272
$^5D_0 \rightarrow {}^7F_4$	14451; 14265; 14204; 14164	14281; 14221; 14192	14524; 14368; 14204	14269; 14225; 14180

(**1**) $[Eu(aind)_3(phen)(H_2O)]$; (**2**) $[Eu(bind)_3(phen)]\cdot H_2O$; (**5**) $[Eu(aind)_3(dmphen)(H_2O)]$; (**6**) $[Eu(bind)_3(dmphen)]\cdot H_2O$.

Table 2. Experimental intensity parameters (Ω_λ = 2.4), radiative (A_{rad}), non-radiative (A_{nrad}) rates, and emission quantum efficiency (η) of the $^5D_0$ emitting level determined for the 2-acyl-1,3-indandionate Eu^{3+}-compounds

Eu^{3+}-complexe	Ω_2 / (10^{-20}cm^2)	Ω_4 / (10^{-20}cm^2)	τ / ms	A_{rad} / s^{-1}	A_{nrad} / s^{-1}	A_{tot} / s^{-1}	η / %
$[Eu(aind)_3(H_2O)_2]$	42.1	14.8	0.108	1532	7739	9261	16.5
$[Eu(aind)_3(tppo)_2]$	35.5	8.9	0.531	1255	628	1883	66.7
$[Eu(aind)_3(phen)(H_2O)]$	4.4	6.6	0.459	280	1897	2177	12.8
$[Eu(aind)_3(dmphen)(H_2O)]$	16.6	3.9	0.229	611	3755	4367	14.0
$[Eu(bind)_3(H_2O)_2]$	40.5	14.2	0.054	1482	17080	18560	8.0
$[Eu(bind)_3(tppo)_2]$	29.4	15.9	0.318	1165	1978	3143	37.1
$[Eu(bind)_3(phen)]\cdot H_2O$	29.5	8.8	0.465	1064	1086	2150	49.5
$[Eu(bind)_3(dmphen)]\cdot H_2O$	25.4	8.6	0.594	950	733	1683.5	56.4

also observed for the other Eu^{3+}-indandionate complexes, as reported in the literature.[11,12] The lower values of A_{nrad} for $[Eu(bind)_3L]\cdot H_2O$ compounds compared to those observed for $[Eu(aind)_3L(H_2O)]$ are a direct consequence of the multiphonon decay, because the water molecule is not coordinated to the Eu^{3+} ion.

Moreover, the luminescence quantum efficiency was determined using the expression $\eta = A_{rad}/(A_{rad} + A_{nrad})$. Table 2 shows that the higher values were observed for the $[Eu(bind)_3L]\cdot H_2O$ compounds than the $[Eu(aind)_3L(H_2O)]$ ones, indicating the absence of water molecules in the first coordination of Eu^{3+} ion, which decrease significantly the luminescence quenching effect.

The experimental intensity parameters Ω_2 and Ω_4 for the complexes were directly determined from the A_{rad} values of the $^5D_0 \rightarrow {}^7F_2$ and $^5D_0 \rightarrow {}^7F_4$ transitions, respectively.[35,36] These parameters depend on the local geometry and the ligating atoms polarizabilities in the first coordinating sphere around the metal central ion.[37] As observed in Table 2, the values of Ω_2 for the complexes containing heteroaromatic phen and dmphen ligands are lower than those ones calculated for the hydrated precursor compounds.[11] This result suggests that the chemical environment polarizabilities have decreased when phen and dmphen ligands substitute water molecules in the first coordination sphere of the Eu^{3+} ion, which have contributed to a significant decrease in the emission rate assigned to the $^5D_0 \rightarrow {}^7F_2$ transition. These values are similar to those found for europium 2-acyl-1,3-indandionate complexes containing triphenylphosphine oxide ligand.[11] The values of Ω_4 exhibit similar behavior, suggesting that the sensibility of the $^5D_0 \rightarrow {}^7F_4$ transition has also been changed with the polarizability and chemical environment.

Conclusions

In the current work, we have reported the synthesis, characterization, and photoluminecent properties of $[Ln(aind)_3L(H_2O)]$ and $[Ln(bind)_3L]\cdot H_2O$ coordination compounds (Ln : Eu^{3+} or Gd^{3+}). The FT-IR data suggest that the water molecule is coordinated to the Ln^{3+} ion in the case of **1**, **3**, **5**, and **7** complexes. The photoluminescence data are consistent with coordination polyhedra calculated via *SPARKLE*/AM1 model for the $[Ln(aind)_3L(H_2O)]$ and $[Ln(bind)_3L]\cdot H_2O$ complexes. The structural differences and the absence of water molecules in the first coordination sphere have great impact on the luminescence quantum efficiency (η) of the Eu^{3+}-complexes, decreasing the luminescence quenching in the intramolecular energy transfer process.

Supplementary Information

The luminescence decay curves of the Eu^{3+}-complexes are available free of charge at http://jbcs.sbq.org.br as PDF file.

Acknowledgements

This research was supported by grants from the Conselho Nacional de Desenvolvimento Científico e Tecnológico (CNPq), Instituto Nacional de Ciência e Tecnologia-Nanotecnologia para Marcadores Integrados (INCT-INAMI), FACEPE-PRONEX, Fundação de Amparo à Pesquisa do Estado de São Paulo (FAPESP No. 2003/07178-8) and, Financiadora de Estudos e Projetos (FINEP).

References

1. Yue, E. W.; Higley, C. A.; DiMeo, S. V.; Carini, D. J.; Nugiel, D. A.; Benware, C.; Benfield, P. A.; Burton, C. R.; Cox, S.; Grafstrom, R. H.; Sharp, D. M.; Sisk, L. M.; Boylan, J. F.; Muckelbauer, J. K.; Smallwood, A. M.; Chen, H.; Chang, C.; Seitz, S. P.; Trainor, G. L.; *J. Med. Chem.* **2002**, *45*, 5233.
2. Sloop, J. C.; Bumgardner, C. L.; Loehle, W. D.; *J. Fluorine Chem.* **2002**, *118*, 135.

3. Enchev, V.; Ivanova, G.; Pavlovic, G.; Rogojerov, M.; Ahmedova, A.; Mitewa, M.; *J. Mol. Struct.* **2003**, *654*, 11.
4. Kilgore, L. B.; Ford, J. H.; Wolfe, W. C.; *Ind. Eng. Chem. Res.* **1942**, *34*, 494.
5. Liu, Y.; Saldivar, A.; Bess, J.; Solomon, L.; Chen, C.; Tripathi, R.; Barrett, L.; Richardson, P. L.; Molla, A.; Kati, W.; Kohlbrenner, W.; *Biochemistry* **2003**, *42*, 8862.
6. Ahmedova, A.; Rusanov, V.; Hazell, A.; Wolny, J. A.; Gochev, G.; Trautwein, A. X.; Mitewa, M.; *Inorg. Chim. Acta* **2006**, *359*, 3123.
7. Ahmedova, A.; Cador, O.; Sorace, L.; Ciattini, S.; Gatteschi, D.; Mitewa, M.; *J. Coord. Chem.* **2008**, *61*, 3879.
8. Ahmedova, A.; Marinova, P.; Stoyanov, N.; Ciattini, S.; Springborg, M.; Mitewa, M.; *Struct. Chem.* **2009**, *20*, 101.
9. Ahmedova, A.; Marinova, P.; Stoyanov, N.; Ciattini, S.; Springborg, M.; Mitewa, M.; *Polyhedron* **2010**, *29*, 1687.
10. Ahmedova, A.; Atanasov, V.; Marinova, P.; Stoyanov, N.; Mitewa, M.; *Cent. Eur. J. Chem.* **2009**, *7*, 429.
11. Teotonio, E. E. S.; Brito, H. F.; Viertler, H.; Faustino, W. M.; Malta, O. L.; Sá, G. F.; Felinto, M. C. F. C.; Santos, R. H. A.; Cremona, M.; *Polyhedron* **2006**, *25*, 3488.
12. Teotonio, E. E. S.; Brito, H. F.; Cremona, M.; Quirino, W. G.; Legnani, C.; Felinto, M. C. F. C.; *Opt. Mater.* **2009**, *32*, 345.
13. Li, J.; Li, H.; Yan, P.; Chen, P.; Hou, G.; Li, G.; *Inorg. Chem.* **2012**, *51*, 5050.
14. Romanova, K. A.; Datskevich, N. P.; Taidakov, I. V.; Vitukhnovskii, A. G.; Galyametdinov, Yu. G.; *Russ. J. Phys. Chem. A* **2013**, *87*, 2108.
15. Greco, C.; Moro, G.; Bertini, L.; Biczysko, M.; Barone, V.; Cosentino, U.; *J. Chem. Theory Comput.* **2014**, *10*, 767.
16. Yang, C. L.; Xu, J.; Li, J. Y.; Lu, M. G.; Li, Y. B.; Wang, X. L.; *Sens. Actuators, B* **2014**, *196*, 133.
17. Yang, C. L.; Xu, J.; Ma, J. Y.; Zhu, D. Y.; Zhang, Y. F.; Liang, L. Y.; Lu, M. G.; *Polym. Chem.* **2012**, *3*, 2640.
18. Bemquerer, M. P.; Bloch, C.; Brito, H. F.; Teotonio, E. E. S.; Miranda, M. T. M.; *J. Inorg. Biochem.* **2002**, *91*, 363.
19. Nakamoto, K.; *Infrared and Raman Spectra of Inorganic and Coordination Compounds, Applications in Coordination, Organometallic, and Bioinorganic*, 6th ed.; Willey: New Jersey, 2009.
20. Gerasimova, T. P.; Katsyuba, S. A.; *Dalton Trans.* **2013**, *42*, 1787.
21. Wagner, C. C.; Baran, E. J.; *Spectrochim. Acta, Part A* **2010**, *75*, 807.
22. Gigante, A. C.; Caires, F. J.; Gomes, D. J. C.; Lima, L. S.; Treu-Filho, O.; Pivatto, M.; Ionashiro, M.; *J. Therm. Anal. Calorim.* **2014**, *115*, 127.
23. Stewart J. J. P. "MOPAC2012", Stewart Computational Chemistry, Colorado Springs, CO, USA. Available: http://OpenMOPAC.net, accessed in April 2014.
24. Freire, R. O.; Rocha, G. B.; Simas, A. M.; *Inorg. Chem.* **2005**, *44*, 3299.
25. Sá, G. F.; Batista, H. J.; Andrade, A. V. M.; Longo, R. L.; Simas, A. M.; Ito, N. K.; Thompson, L. C.; *Inorg. Chem.* **1998**, *37*, 3542.
26. Li, X.; Bian, Z.; Jin, L.; Lu, S.; Huang, S.; *J. Mol. Struct.* **2000**, *522*, 117.
27. Chen, X.-F.; Zhu, X.-H.; Xu, Y.-H.; Raj, S. S. S.; Öztürk, S.; Fun, H.-K.; Ma, J.; You, X. Z.; *J. Mater. Chem.* **1999**, *9*, 2919.
28. Lü, Y.-G.; Li, G.; Shi, C.-H.; Yu, L. S.; Luan, F.; Zhang, F. J.; *Trans. Nonferrous Met. Soc. China* **2010**, *20*, 2336.
29. Yu, X.; Su, Q.; *J. Photoch. Photobio. A* **2003**, *155*, 73.
30. Brito, H. F.; Malta, O. L.; Felinto, M. C. F. C.; Teotonio, E. E. S. In *The Chemistry of Metal Enolates*, v. 1; Zabicky, J., ed.; John Wiley & Sons, Ltd.: Chichester, 2009, ch. 3.
31. Binnemans, K.; *Chem. Rev.* **2009**, *109*, 4283.
32. Gruber, J. B.; Valiev, U. V.; Burdick, G. W.; Rakhimov, S. A.; Pokhrel, M.; Sardar, D. K.; *J. Lumin.* **2011**, *131*, 1945.
33. Forsberg, J. H.; *Coord. Chem. Rev.* **1973**, *10*, 195.
34. Sá, G. F.; Malta, O. L.; Donegá, C. M.; Simas, A. M.; Longo, R. L.; Santa-Cruz, P. A.; Silva Júnior, E. F.; *Coord. Chem. Rev.* **2000**, *196*, 165.
35. Faustino, W. M.; Nunes, L. A.; Terra, I. A. A.; Felinto, M. C. F. C.; Brito, H. F.; Malta, O. L.; *J. Lumin.* **2013**, *137*, 269.
36. Werts, M. H. V.; Jukes, R. T. F.; Verhoeven, J. W.; *Phys. Chem. Chem. Phys.* **2002**, *4*, 1542.
37. Bünzli, J.-C. G.; Eliseeva, S. V. In *Lanthanide Luminescence: Photophysical, Analytical and Biological Aspects VII*; Hänninen, P.; Härmä, H., eds.; Springer: Berlin, 2010, ch. 1.

Submitted on: March 13, 2014
Published online: August 26, 2014

FAPESP has sponsored the publication of this article.